Measurement of the B_c Lifetime in $B_c \to J/\psi + l + X$ Decays

The CDF Collaboration[1]

[1] *URL http://www-cdf.fnal.gov*

(Dated: April 28, 2008)

We measure the B_c^+ lifetime in 1 fb^{-1} of inclusive $J/\psi \to \mu\mu$ data collected with the CDF II detector using $B_c^\pm \to J/\psi + l^\pm + X$ decays, where l can be an electron or a muon and X are unmeasured particles. We analyze $J/\psi + l$ candidates with an invariant mass between 4 and 6 GeV/c^2, which is the range in which we expect the B_c signal to lie. A variety of backgrounds are present in the $J/\psi + l$ signal mass window and we estimate the contribution of these backgrounds to the lifetime using both data and Monte Carlo simulation. We perform an extended log likelihood fit of the $J/\psi + l$ lifetime and find an average lifetime of the B_c meson of $c\tau = 142.5\,^{+15.8}_{-14.8}$ (stat.) $\pm$ 5.5 (syst.) μm.

PACS numbers: 13.20.He, 14.40.Nd, 14.65.Fy

I.   INTRODUCTION

The B_c^+ is the bound state of a $\bar{b}$ and c quark. Its properties are of interest for a number of reasons:

- The quark composition of the meson makes it an interesting laboratory for studying QCD, since the $\bar{b}$ and c quark are much closer in mass than more commonly studied heavy-light mesons, such as the B^0, B^+, or B_s^0 mesons.

- The B_c total width can have significant contributions from the partial widths of the c-quark decay, the b-quark decay, or annihilation of the b and c quarks to a W meson, in contrast to the light B mesons, where the b quark decay is expected to dominate the width. Consequently, the B_c is predicted to have a lifetime of $c\tau = 165 \pm 45$ μm [1], which is considerably shorter than the average light B meson lifetime of ≈ 450 μm [2].

Decays of the B_c through the b quark are of particular interest, since weak decays to a lepton and neutrino, $b \to c+l+\nu_l$, will be common and lead to semileptonic final states with a $c\bar{c}$, which can form a J/ψ meson. Theory predicts a branching fraction for $B_c \to J/\psi + l + X$ of $\sim 2\%$ [1]. We choose to use this semileptonic decay channels in the measurement of the B_c meson lifetime because:

- The CDF trigger system includes triggers for $J/\psi \to \mu^+\mu^-$ events that do not introduce biases into the lifetime of events.

- The predicted branching fraction for $B_c \to J/\psi + l + X$ is large compared to the branching fraction for $B_c \to J/\psi + \pi$.

- The contributions of $J/\psi + l$ from other B-hadron decays or $c\bar{c}$ are expected to be small enough that an excess of signal can be measured.

This note describes a measurement of the B_c meson lifetime using decays with $J/\psi + l + X \to \mu^+\mu^- + l + X$ in the final state where X are undetected particles. The B_c mesons are produced in $p\bar{p}$ collisions at $\sqrt{s} = 1.96$ TeV at the Fermilab Tevatron and the data are collected with the CDF II detector. The CDF II detector is described in detail in [3].

A.   Measuring Lifetimes

To measure the lifetime of the B_c, we construct a per event lifetime that is defined using variables measured in the transverse plane. If all of the decay products of the B_c decay are identified, the lifetime ct, which is the lifetime of the B_c meson in its rest frame measured in units of microns of light travel time, and is expressed as

$$ct = \frac{mL_{xy}}{p_T} \tag{1}$$

where m is the mass of the B_c, p_T is the momentum of the B_c in the plane transverse to the direction of the proton beam, and L_{xy} is the decay length of the B_c projected along the transverse momentum. The mass of the B_c used in this measurement is $m = 6.286$ GeV/c^2 [4]. However, we do not measure all of the particles in the B_c final state, so we must define a new lifetime

$$ct^* = \frac{mL_{xy}(J/\psi l)}{p_T(J/\psi l)} \tag{2}$$

where L_{xy} and p_T are evaluated using the $J/\psi + l$ system. We can obtain the true B_c lifetime by defining a factor K, where $ct = Kct^*$. We evaluate the K factor distribution, $H(K)$, for B_c events using Monte Carlo simulation. We are then able to express the distribution of ct^* for $B_c \to J/\psi + l + X$ as

$$F_{bc}(ct^*, \sigma) = \int dK H(K)\frac{K}{c\tau}\theta(ct^*)exp(-\frac{Kct^*}{c\tau}) \otimes \frac{1}{\sqrt{2\pi}s\sigma}e^{-\frac{1}{2}(\frac{ct^*}{s\sigma})^2} \tag{3}$$

where $c\tau$ us the average B_c lifetime and σ represents the estimated error on the measurement of ct^* for each event.
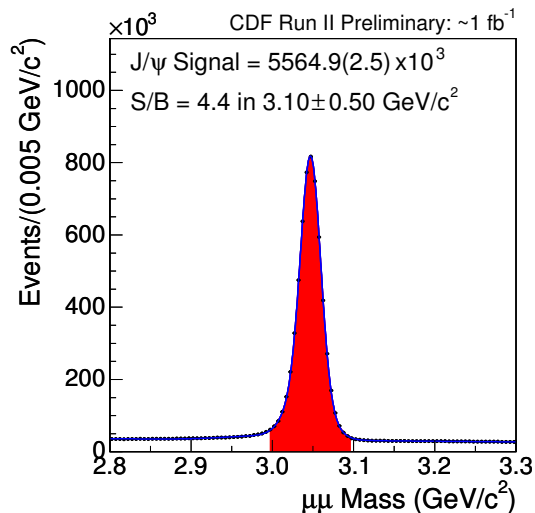
FIG. 1: Invariant mass of di-muon candidates with J/ψ signal candidates selected from the red filled region.

B. Lifetime Fitting Procedure

The measurement of the B_c average lifetime will be carried out by minimizing $-2Log(L)$, which is evaluated for the candidate $J/\psi + l$ events. L is the likelihood function for the ct^* and σ measured in candidate events and includes the $c\tau$ as a free parameter. L also includes terms for the signal component (see previous section) and background components, which will be discussed in subsequent sections.

The minimization of $-2Log(L)$ is carried out separately for the $J/\psi + \mu$ and $J/\psi + e$ final states, since the background models differ between the two channels. We sum $-2Log(L)$ for the two channels to obtain the average $B_c \to J/\psi + l$ lifetime.

II. DATA SAMPLE & EVENT SELECTION

This analysis is done using ~ 1 fb^{-1} of data collected with the CDF II detector. The events are collected using a trigger that selects di-muon candidates of two types:

1. Two muons with $p_T > 1.5$ GeV/c and hits in the central muon detector (CMU) [5], which covers $|\eta| < 0.6$.

2. One muon with $p_T > 1.5$ GeV/c and hits in the CMU and a second muon with $p_T > 2.0$ GeV/c and hits in the central muon extension detector (CMX), which covers $0.6 < |\eta| < 1.0$.

Events with a di-muon mass that falls within a ± 50 MeV/c^2 window around $m_{J/\psi} = 3.097$ GeV/c^2 are selected. These events can be seen in Fig. 1. A multi-wire drift chamber (COT) and silicon micro-strip detector, which consists of the Silicon Vertex Tracker II (SVX II) [7] and Intermediate Silicon Layers (ISL) [8], provide precision measurements of the particle momenta that are necessary to accurately reconstruct the particle system masses.

We also require that a third lepton (either a muon or an electron) forms a vertex with the J/ψ candidate and that the vertex has a probability > 0.001. The measurement of particle positions near the interaction point, which is necessary for vertexing as well as for measuring ct^*, are carried out using the SVX II and ISL.

The third leptons are identified as follows:

- Muons - Particles with $p_T > 3.0$ GeV/c^2 and hits in the CMU and central muon upgrade detector (CMP) detectors. A cut on the energy loss per unit path length traveled, dE/dx, is also applied to reduce the number of fake muons in the analysis.

- Electrons - Particles with $p_T > 2.0$ GeV/c^2 are identified as electrons using a likelihood ratio

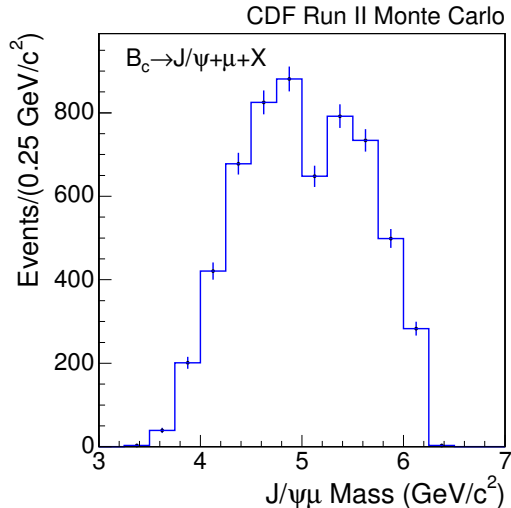$$L_r = \frac{L_e}{L_e + L_\pi} \tag{4}$$

FIG. 2: Mass of $J/\psi + \mu$ system for simulated $J/\psi + \mu$ events from B_c decays.

where L_e and L_π are the likelihoods that a track is an electron or pion, respectively, based on information from the electromagnetic and hadronic calorimeters. As with the muons, we cut on $\mathrm{d}E/\mathrm{d}x$ to reduce the number of hadrons faking electrons.

Monte Carlo simulation of $B_c \to J/\psi + \mu + X$ events, shown in Fig. 2 indicate that the $J/\psi + \mu$ mass peak is quite broad. We select events with $4.0 < m_{J/\psi+l} < 6.0 \text{ GeV}/c^2$, which includes almost all of the expected signal, but excludes significant amounts of background.

III. BACKGROUNDS

The broad $J/\psi + l$ mass peak expected for signal events means we cannot rely on the mass sidebands as a way to estimate our backgrounds. Instead, we consider the expected backgrounds from a number of sources and use data-driven methods to estimate them where possible and Monte Carlo simulation where no data-driven method is apparent.

Since the production rate of B_c meson relative to the lighter B mesons is very small, we expect relatively rare combinations in $b\bar{b}$ and $c\bar{c}$ events to contribute significantly to the $J/\psi + l$ background. The expected backgrounds are:

1. Fake Lepton - Events with a J/ψ from $b\bar{b}$ or $c\bar{c}$ and an additional long lived hadron (π, K or p). The hadron can fake a muon by punching through to the muon chambers or by decaying to a muon before it reaches muon chambers. It can fake an electron by leaving a signature in the calorimetry that looks sufficiently like an electron to pass the electron likelihood ratio cut.

2. Fake J/ψ - Events from the continuum background for J/ψ that also have a third lepton in them.

3. $b\bar{b}$ - Events with a J/ψ from one b-quark jet and a lepton from the other. The probability to make a vertex is low, but $\sim 10\%$ of B decays with J/ψ in the final state will have a lepton in the opposite jet.

4. Residual e^+e^- - Unique to the $J/\psi + e$ channel are events where an electron is produced as part of an e^+e^- pair, either by photon conversion or by decay of a light meson such as a π^0 or η. We attempt to veto these events by identifying the other electron in the pair, but a residual background remains because the veto efficiency is less than 1.

5. Prompt J/ψ - Events in which a J/ψ is produced at the primary interaction point and is combined with a third lepton.

Table I summarizes the background estimates for the $J/\psi + \mu$ and $J/\psi + e$ channels, compared to the number of candidate events. We describe the methods for estimating each background in detail in the following sub-sections.

Background Type	$J/\psi + \mu$	$J/\psi + e$
Fake Lepton	96.1 ± 4.6	312.0 ± 4.1
Fake J/ψ	141.5 ± 8.4	325.2 ± 10.0
$b\bar{b}$	77.5 ± 7.9	222.5 ± 11.2
Residual Conversion	-	416.8 ± 41.5
Background Subtotal	315.1 ± 12.4	1276.5 ± 44.3
Candidates	572	1935

TABLE I: Number of background events estimated for each background type. The excess of candidate events over the background estimates is expected and attributed to B_c signal events and the prompt J/ψ background.

A. Fake Lepton Background

We model the fake lepton background by starting with our $J/\psi + l$ samples and removing the lepton requirements from the third particle. We call this the $J/\psi + track$ sample. Each of the hadrons in this sample is a candidate to fake a lepton. If we estimate the probability that each of these hadrons is a particular particle, F_π, F_K, or F_p, and the probability for a given particle type to fake a lepton, P_π, P_K, or P_p, we can estimate a total fake lepton probability for each event that can be used to weight the events in the $J/\psi + track$ sample. The weighting for a given event can be written as

$$W = F_\pi P_\pi + F_K P_K + F_p P_p. \tag{5}$$

Once this weight is determined, the background of fake lepton events in the final signal sample can be determined.

The particle type composition of the third tracks in the $J/\psi + track$ is estimated using dE/dx and time of flight (TOF) [9] information. Figures 3 and 4 show the measured particle fractions, which are an estimate of the probability that a given track is a certain hadron, as a function of the third track momentum and the ct^* of the event for the $J/\psi + \mu$ and $J/\psi + e$ channels, respectively.

The probabilities for hadrons to fake leptons can be estimated using samples in which the hadrons are identified as decay products in relatively pure and fully reconstructed systems. For kaons and pions, we look at the decay chain $D^{*+} \to D^0 + \pi^+ \to \pi^+ + K^- + \pi^+$ and the charge-conjugate decay. The sign the pion from the $D^{*\pm}$ meson decay identifies the pion and kaon from the D^0 meson decay. We identify a sample of protons by reconstructing the $\Lambda \to p^+ + \pi^-$ decay and its charge conjugate. In this decay the proton always has a larger momentum than the pion, given the selection cuts.

We reconstruct and fit the D^0 and Λ mass peaks in two cases: (a) the pion, kaon, or proton track has no lepton selection applied to it, and (b) the pion, kaon, or proton track is required to pass the lepton selection discussed in Section II. The ratio of events under the mass peak for these two cases gives an estimate of the fake lepton probability. Figure 5 shows examples of the mass fits. The fake rates for the muons and electrons are summarized in Fig. 6.

The ct^* for fake muon and fake electron backgrounds are shown in Fig. 7 and the estimated number of background events are 96.1 ± 4.6 and 312.0 ± 4.1 for $J/\psi + \mu$ and $J/\psi + e$, respectively.

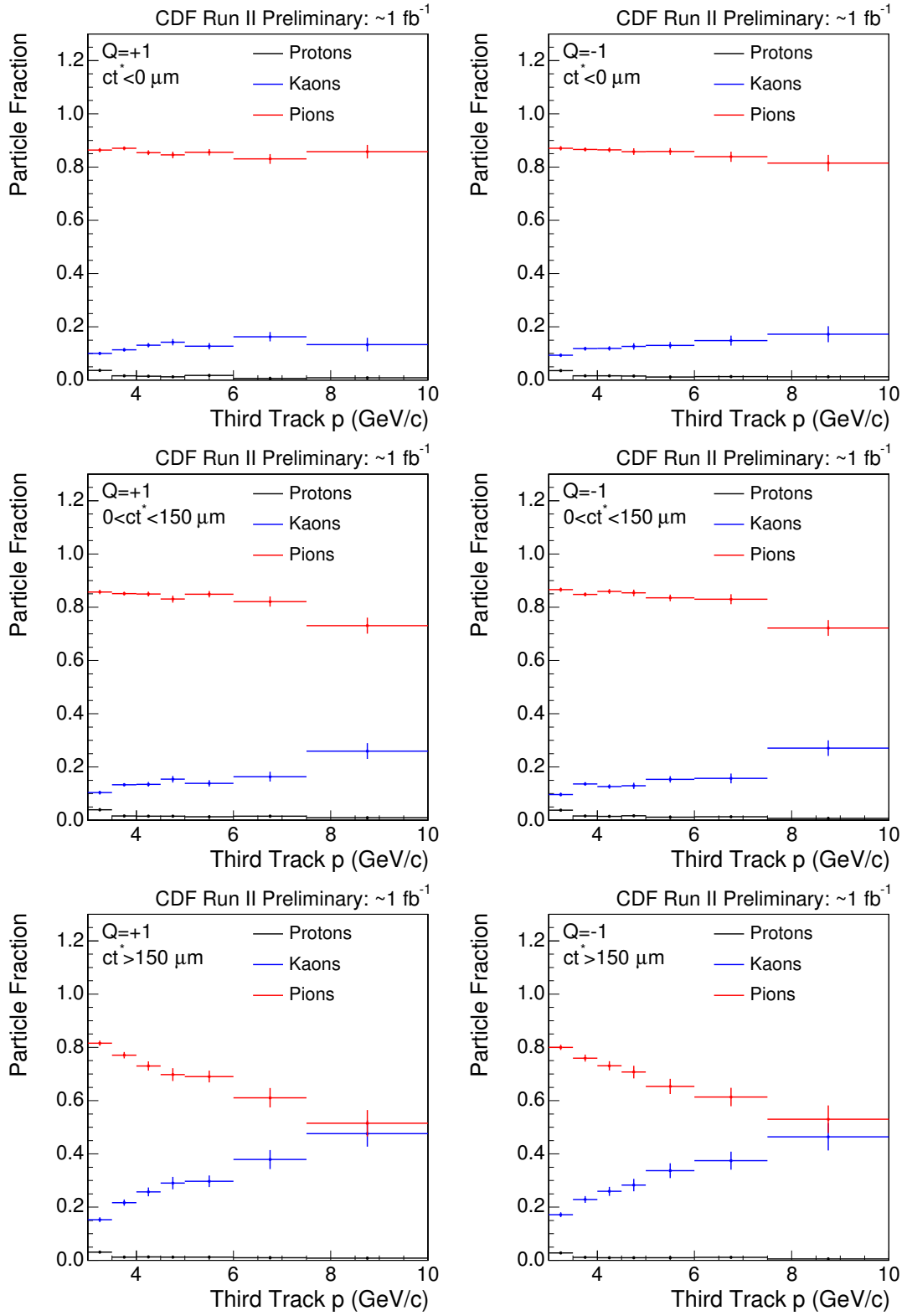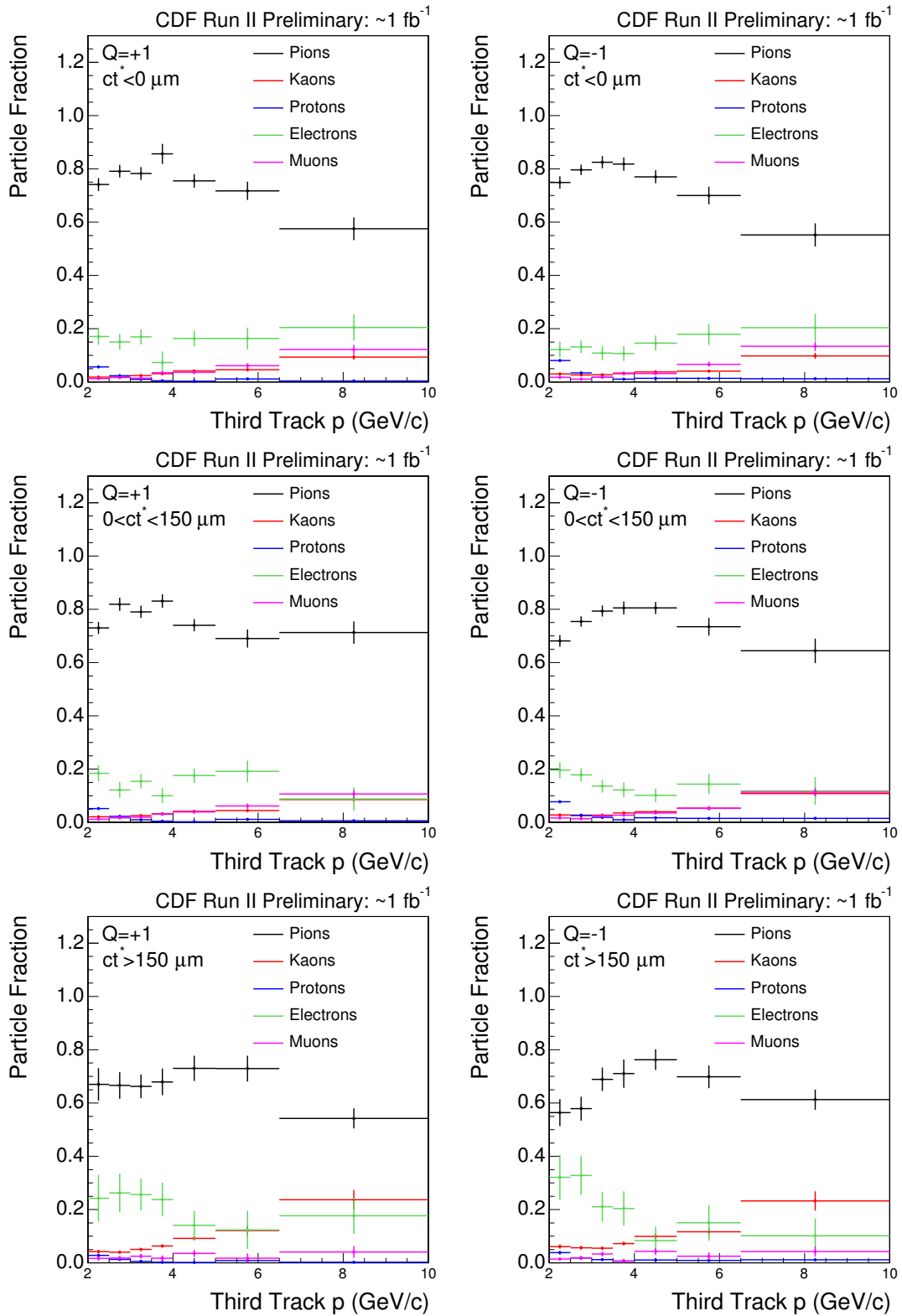FIG. 3: Particle fractions for third tracks in the J/ψ+track (muon requirement removed) sample as a function of the third track momentum. Left are positive charge, right are negative charge. Top row is $ct^* < 0$ μm, middle row is $0 < ct^* < 150$ μm and bottom row is $ct^* > 150$ μm.
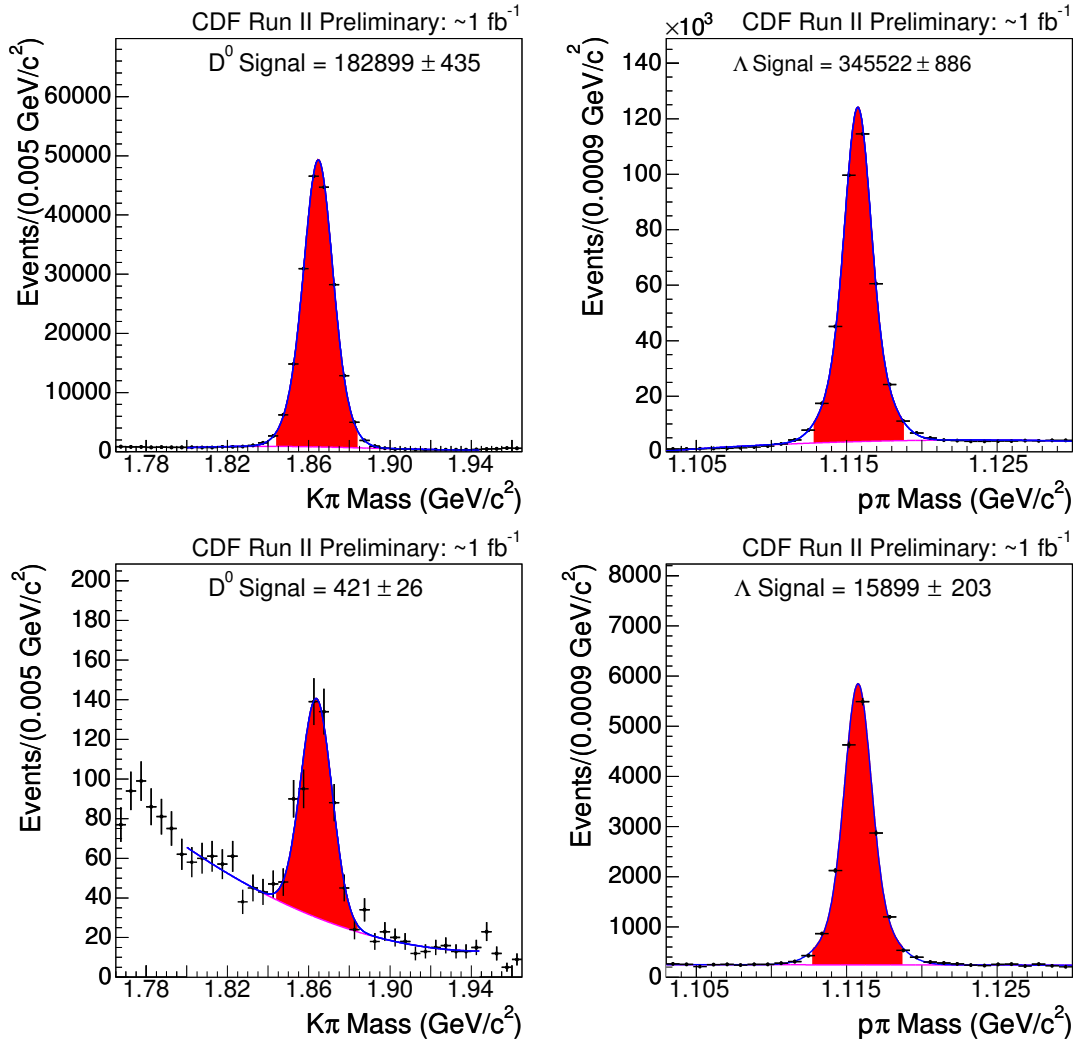
FIG. 4: Particle fractions for third tracks in the J/ψ+track (electron requirement removed) sample as a function of the third track momentum. Left are positive charge, right are negative charge. Top row is $ct^* < 0$ μm, middle row is $0 < ct^* < 150$ μm and bottom row is $ct^* > 150$ μm.

FIG. 5: Examples of fits of D^0 (left) and Λ (right) masses used to estimate fake rates. Top: the tracks associated with the $\pi^\pm$ and p^- decay products do not have any lepton identification requirements applied. Bottom: the $\pi^\pm$ and p^- tracks are required to be identified as leptons.
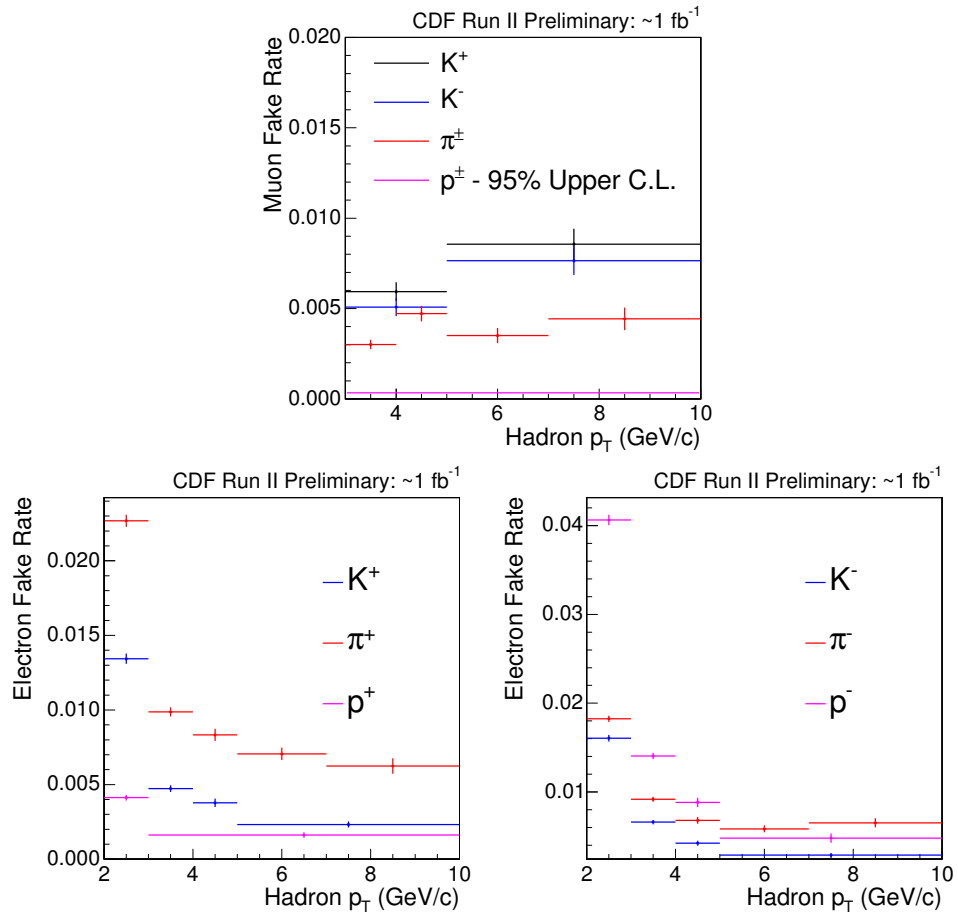
FIG. 6: Hadron faking muon probabilities as a function of hadron p_T (top). Hadron faking electron probabilities as a function of hadron p_T for positively charged hadrons (bottom left) and negatively charged hadrons (bottom right).
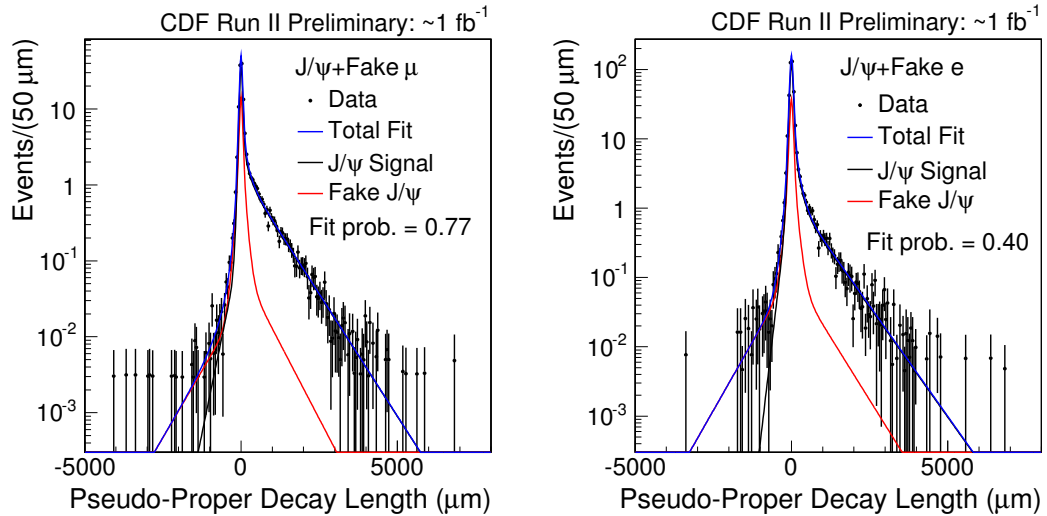
FIG. 7: Fitted ct^* distributions for $J/\psi + track$ events weighted by fake lepton probabilities. The contribution from fake J/ψ is modeled using sidebands and accounted for by the red curve. The estimate of the fake muon background is shown on the left, while the estimate of fake electron background is shown on the right.
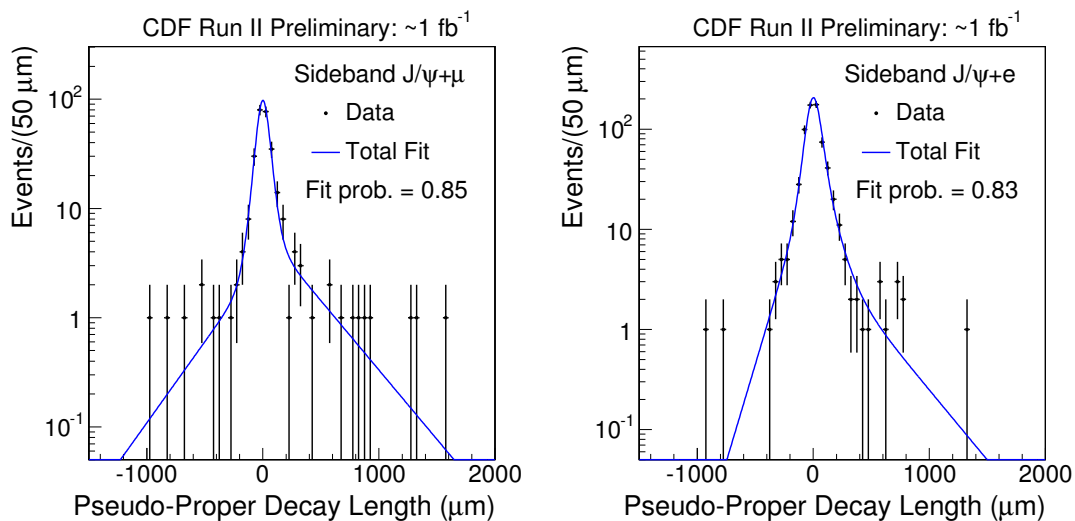
FIG. 8: Fitted ct^* distributions for sideband $J/\psi + l$ events for the $J/\psi + \mu$ channel (left) and the $J/\psi + e$ channel (right).

B. Fake J/ψ Background

The fake J/ψ background is modeled using events from the di-muon mass sidebands in the $J/\psi + l$ samples. Events are selected by requiring $100 < |m_{\mu\mu} - 3097| < 200$ MeV/c^2. The fitted ct^* distributions for the $J/\psi + \mu$ and $J/\psi + e$ channels can be seen in Fig. 8. The estimated number of background events is 141.5 ± 8.4 and 325.2 ± 10.0 for the $J/\psi + \mu$ and $J/\psi + e$ channels, respectively.

C. $b\bar{b}$ Background

The $b\bar{b}$ background is modeled using a Monte Carlo sample of events generated with Pythia. The parton distribution model used is CTEQ5L and the events are generated in the QCD jets mode that allows tree level $2 \to 2$ processes, where the inclusion of initial and final state QCD radiation gives multi-jet events [10]. We categorize the generated $b\bar{b}$ events by the QCD process by which they are created:

- Flavor Creation (FC) - $q\bar{q} \to b\bar{b}$ or $gg \to b\bar{b}$. The $b\bar{b}$ will typically be back to back.

- Flavor Excitation (FE) - Scattering of an off-mass shell b quark in the initial state to give an on-shell $b\bar{b}$ pair in the final state. The opening angle between $b\bar{b}$ pairs can be smaller than it is for FC.

- Gluon Splitting (GS) - Scattering of a gluon that splits to a $b\bar{b}$ pair. The opening angle for the $b\bar{b}$ can be small.

Our model of the $J/\psi + l$ background is sensitive to the relative amounts of FC, FE and GS present in our Pythia sample. We tune the Pythia sample by looking at a $b\bar{b}$ correlation that we expect to be different for the three QCD processes, specifically the azimuthal angle between the J/ψ and the third μ, $\Delta\phi$, for events where there is no vertex probability cut on the three particle system. We fit the Pythia-predicted $\Delta\phi$ distributions of the FC, FE, and GS to the $\Delta\phi$ distribution in data, allowing the relative amounts of the QCD processes to be determined by the fit. The fitted data can be seen in Fig. 9. We use this tuning in our model of the $b\bar{b}$ background.

After tuning our Pythia sample using the $J/\psi + \mu$ $\Delta\phi$ distribution, we carry out an additional check against the data using the impact parameter of the third lepton with respect to the J/ψ vertex, $d_0^{J/\psi}$. Once again, we do not apply a vertex probability cut to the three track system, which enhances the contribution of $b\bar{b}$ events. We expect the $d_0^{J/\psi}$ distribution to be dominated by $b\bar{b}$ events at large values, since the third lepton and J/ψ do not originate from the same vertex. Figure 10 shows the background estimates for $d_0^{J/\psi}$ compared to data. We see good agreement in all bins except the first two, where we expect an excess due to B_c signal events.

We model the ct^* distribution due to $b\bar{b}$ using our tuned Pythia sample and the fitted distributions for $J/\psi + \mu$ and $J/\psi + e$ events can be seen in Fig. 11. The number of $b\bar{b}$ $J/\psi + l$ events in the Pythia sample is measured relative to
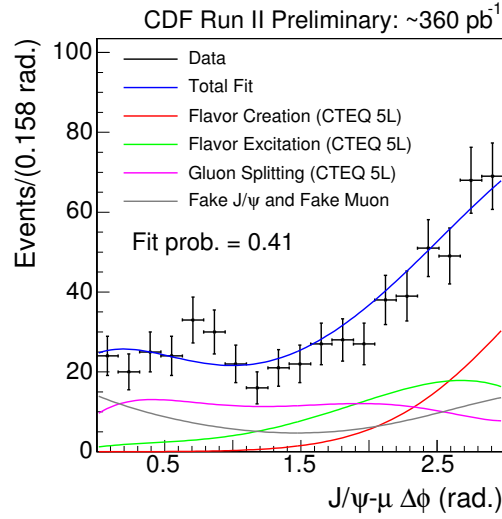
FIG. 9: Fitted $J/\psi\mu\ \Delta\phi$ for events with not vertex probability cut on the three particle system. The relative fractions of flavor creation, gluon splitting and flavor excitation are free parameters in the fit.
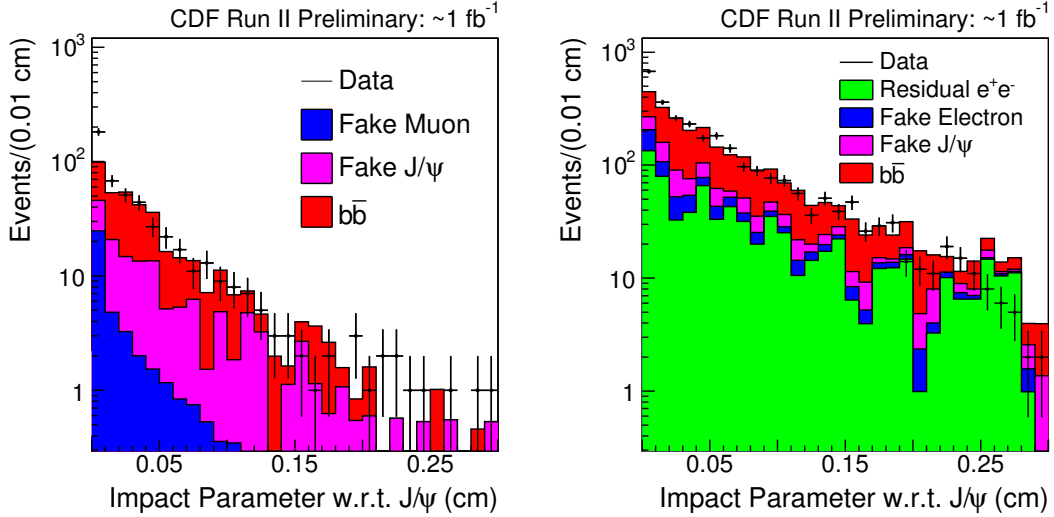

FIG. 10: Distributions of the impact parameter of the third lepton with respect to the J/ψ vertex for $J/\psi + l$ events with no vertex probability cut applied. We expect an excess in the first two bins from B_c signal events.

the fitted $B^\pm \rightarrow J/\psi + K^\pm$ mass peak. This ratio is multiplied by the events in the $B^\pm \rightarrow J/\psi + K^\pm$ mass peak in data to give an estimate of the $b\bar{b}$ background in data. We estimate 77.5 ± 7.9 and 222.5 ± 11.2 background events for the $J/\psi + \mu$ and $J/\psi + e$ channels respectively.

D.   Residual e^+e^- Background

As mentioned previously, we remove events where the electron originates from the production of an e^+e^- pair by identifying the partner track, whether by photon conversion or decay of light neutral mesons such as the π^0. Since the efficiency for reconstructing the partner track is less than 1, there is a residual background of events that are not vetoed. Since we know the number of vetoed events N_{veto}, we can model the number of residual background events
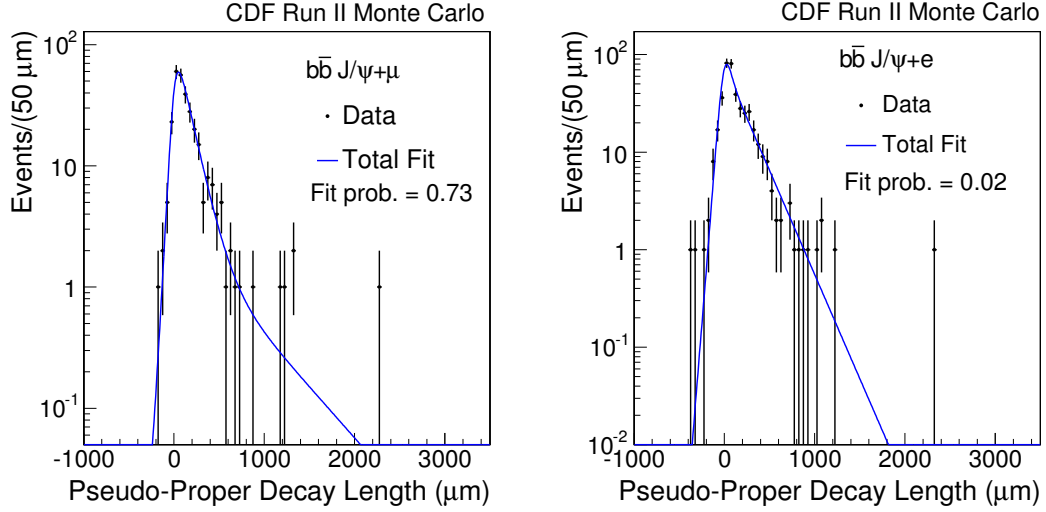
FIG. 11: Fitted ct^* distributions for $J/\psi + l$ events from $b\bar{b}$ for $J/\psi + \mu$ (left) and $J/\psi + e$ (right).

N_{res}, if we know the efficiency for vetoing e^+e^- pairs, ϵ_{veto}. The formula that relates N_{res} to N_{veto} is

$$N_{res} = \frac{(1 - \epsilon_{veto})}{\epsilon_{veto}} N_{veto} \tag{6}$$

We use a Pythia sample of B meson decays with a J/ψ in the final state to estimate ϵ_{veto} for e^+e^- pairs in events that pass our $J/\psi + e$ selection. The efficiency is calculated separately for e^+e^- from photon conversion and light neutral meson decays, and can be seen in Fig. 12. Applying the above formula to the sample of vetoed events, we find the expected ct^* distribution for residual e^+e^- events, which is shown with the fit overlaid in Fig. 13. The estimated number of residual e^+e^- events is 416.8 ± 41.5.
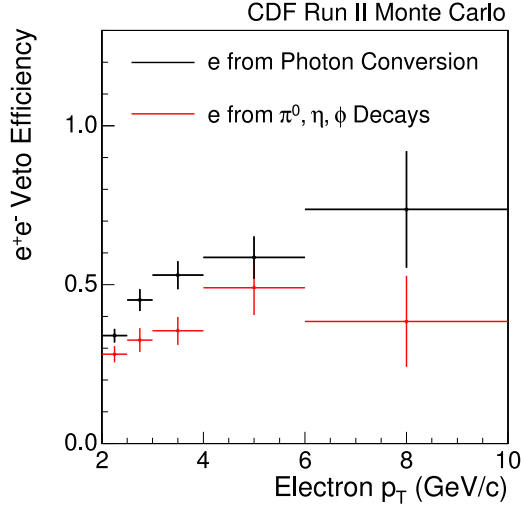
FIG. 12: Efficiency for vetoing e^+e^- events, evaluated using a Pythia sample of B hadron decays with J/ψ among the decay products.
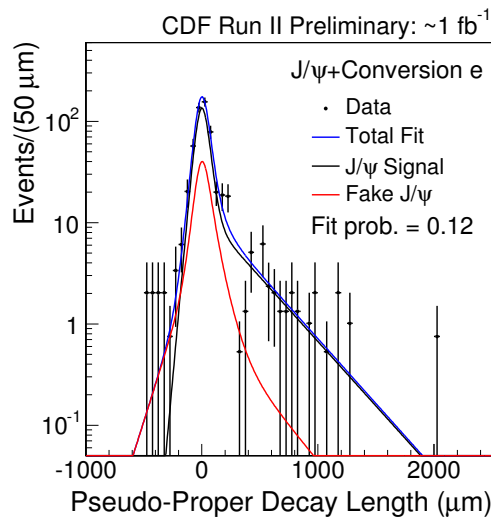
FIG. 13: Fitted ct^* of vetoed e^+e^- events that are weighted by $(1-\epsilon_{veto})/\epsilon_{veto}$ to give the ct^* estimate of residual e^+e^- events.

	Fraction of $J/\psi + l + X$ Events		
Decay	Input to Simulation	After $J/\psi + \mu$ Selection	After $J/\psi + e$ Selection
$J/\psi l\nu_l$	0.8581	0.9710	0.9629
$J/\psi \tau\nu_\tau$	0.0370	0.0085	0.0114
$\psi(2S)l\nu_l$	0.0235	0.0164	0.0187
$B_s l\nu_l$	0.0226	0.0000	0.0002
$B_s^* l\nu_l$	0.0271	0.0000	0.0000
$B^0 l\nu_l$	0.0009	0.0000	0.0000
$B^{0*} l\nu_l$	0.0018	0.0000	0.0000
$J/\psi D_s$	0.0054	0.0010	0.0014
$J/\psi D_s^*$	0.0217	0.0028	0.0041
$J/\psi D^0$	0.0005	0.0000	0.0002
$J/\psi D^{0*}$	0.0014	0.0001	0.0002

TABLE II: Estimates of the fraction of $J/\psi + l$ events from different B_c decays, where the input to the $J/\psi + l$ final states include all branching ratios to intermediate states.

E. Prompt J/ψ Background

There are additional events with a prompt J/ψ and a third lepton that are not modeled by any of the other backgrounds. We do not attempt to estimate the total number of these events. Instead, we allow the normalization to float freely in the B_c lifetime fit. The ct^* distribution for these events is modeled using a single Gaussian, which we find to be a good model of the experimental resolution for ct^* measurements.

IV. SIGNAL MODEL

As mentioned in Section I A, we need to use K factors that account for the unmeasured momentum in the $J/\psi + l$ final states in order to parameterize the ct^* distribution for signal events with the average B_c lifetime $c\tau$. We study the K factors using a Monte Carlo simulation of B_c decays, where all decays with $J/\psi + l$ in the final state have been included. Table IV lists the relative branching fractions used in the Monte Carlo, which come from theoretical calculations [1]. The resulting K factor distributions for $J/\psi + l$ events in the Monte Carlo sample are shown in Fig. 14.
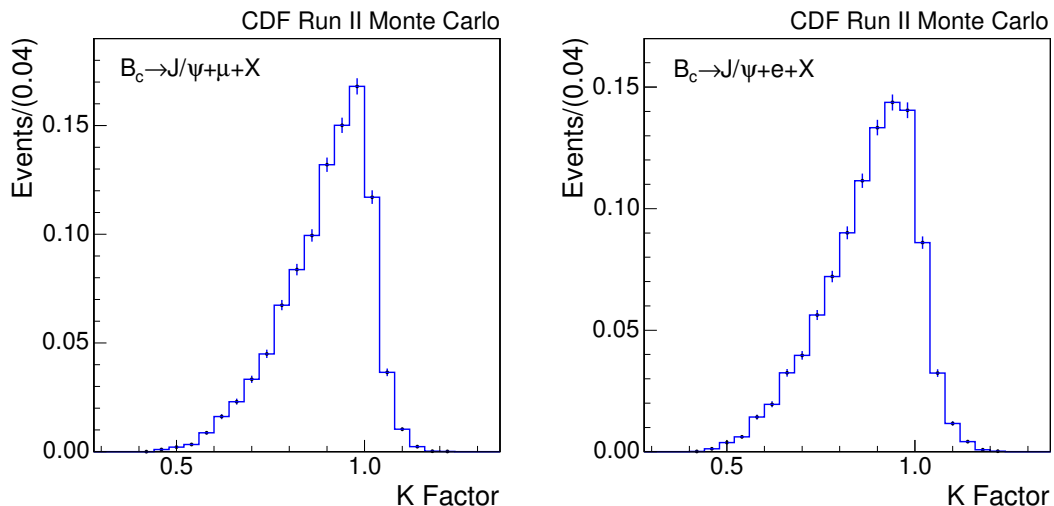
FIG. 14: K factors for $B_c \to J/\psi + l + X$ decays estimated using a Monte Carlo simulation of signal events for $J/\psi + \mu$ (left) and $J/\psi + e$ (right).

V. SYSTEMATIC UNCERTAINTIES

The systematic uncertainties in the B_c lifetime measurement originate from uncertainties in our models for background and signal events. Some of the largest systematic uncertainties are:

- Resolution Function - The ct^* dependence of signal events and prompt J/ψ background events are not explicitly determined from any data or Monte Carlo samples. In both of these models we include a smearing by a single Gaussian function that represents the experimental resolution for measuring ct^*. For an estimate of the systematic uncertainty due to this choice, we consider a more complex two Gaussian resolution function. The uncertainty in the choice of resolution function adds an uncertainty to the lifetime measurement of 3.8 μm.

- Pythia Model for $b\bar{b}$ - As discussed previously, we generate a Pythia sample to model the $b\bar{b}$ background, tuning the sample to match data using the $\Delta\phi$ correlation for unvertexed $J/\psi + \mu$ events. If we assume that the tuning is unnecessary, we can estimate the systematic uncertainty related to our Pythia tuning. We find this leads to a 2.4 μm uncertainty in the lifetime measurement.

- Silicon Detector Alignment - Uncertainties related the the exact position for sensors in the the SVX II and ISL silicon detectors introduce an uncertainty in the measured lifetime which is 2.0 μm.

- Residual e^+e^- Estimate - We estimate the residual e^+e^- background using an ϵ_{veto} which is obtained from a Pythia Monte Carlo simulation. This sample may not perfectly model the ϵ_{veto} which is present in data. The uncertainty in estimating ϵ_{veto} introduces a 1.5 μm uncertainty in the lifetime measurement.

- B_c Spectrum - We use a Monte Carlo sample to model the K factor distribution of B_c events. We must make assumptions about the B_c momentum spectrum when generating this Monte Carlo sample. Uncertainties related to the B_c momentum spectrum introduce a 1.3 μm uncertainty in the measured B_c lifetime.

Table V summarizes the systematic uncertainties for the B_c lifetime measurement. We add the individual uncertainties in quadrature to obtain a total uncertainty of 5.5 μm.

VI. RESULTS

We fit the ct^* distributions for signal candidates in the $J/\psi + \mu$ and $J/\psi + e$ channels separately using likelihood functions based on our models for signal and background events. The fitted data can be seen in Fig. 15 and Fig. 16.

Description	Uncertainty (μm)
bb Pythia Settings	2.4
Monte Carlo Tracking Resolution	0.7
B_c Spectrum	1.3
B_c Branching Fractions	0.5
B_c σ Model	0.4
Fake J/ψ ct^* Model	0.8
Resolution Function	3.8
Silicon Alignment	2.0
Fake Electron Estimate	0.2
e^+e^- Veto Efficiency	1.5
Fake Muon Estimate	0.6
Fake J/ψ Normalization	0.4
Total in Quadrature	5.5

TABLE III: Systematic uncertainties in the measurement of the B_c lifetime.

The fitted lifetimes for the individual channels are

$$c\tau_\mu = 179.1^{+32.6}_{-27.2} \text{ (stat.)} \ \mu\text{m},$$ (7)
$$c\tau_e = 121.7^{+18.0}_{-16.3} \text{ (stat.)} \ \mu\text{m}.$$

To obtain a combined lifetime from the $J/\psi+l$ samples, we take the sum $-2Log(L_e)-2Log(L_\mu)$, which is equivalent to multiplying the likelihood for the individual channels. We evaluate $-2Log(L_e)$ and $-2Log(L_\mu)$ as a function of the B_c lifetime by fixing the B_c lifetime at varying values and minimizing the rest of the parameters in the fit. The resulting likelihood scans of the B_c lifetimes and their sum can be seen in Fig. 17. The lifetime we extract from the minimum of the combined likelihood is

$$c\tau = 142.5^{+15.8}_{-14.8} \text{ (stat.)} \pm 5.5 \text{ (syst.)} \ \mu\text{m}.$$ (8)

Figure 18 shows a our average of the CDF Run I B_c lifetime [11], the most recent D0 Run II B_c lifetime [12], and the result presented in this paper. The lifetimes are weighted by the total variance of the individual measurements in the average.
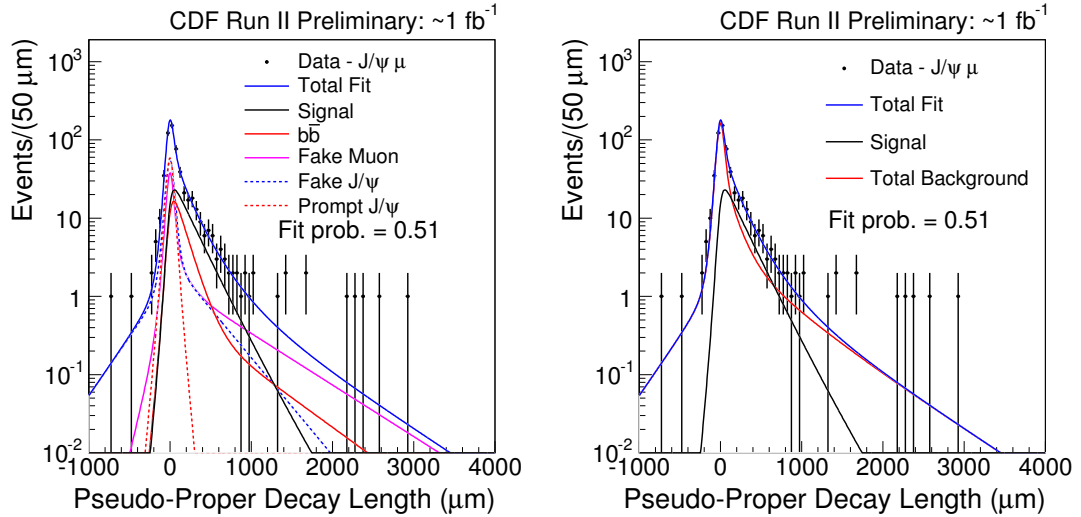

FIG. 15: Fitted ct^* for $J/\psi + \mu$ candidate events, where backgrounds are shown broken into individual components (left) and combined into a single component (right).
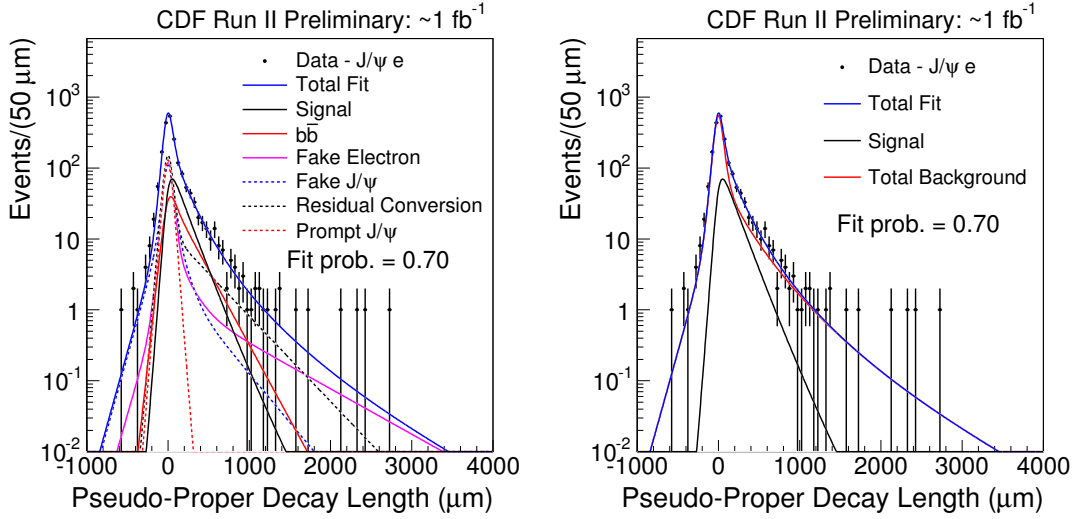
FIG. 16: Fitted ct^* for $J/\psi + e$ candidate events, where backgrounds are shown broken into individual components (left) and combined into a single component (right).
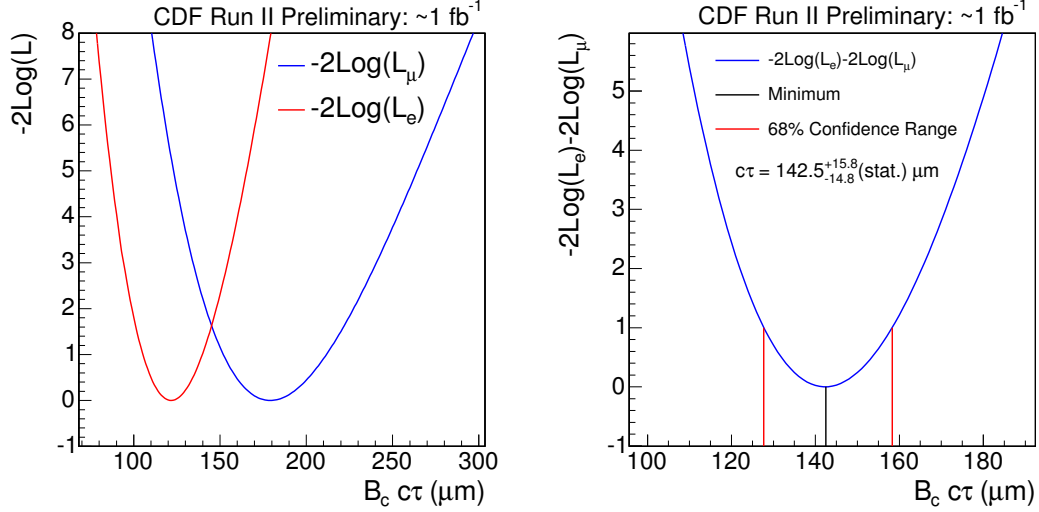

FIG. 17: $-2Log(L)$ as a function of the $B_c\ c\tau$ for both channels (left) and $-2Log(L_e) - 2Log(L_\mu)$ (right). The minimum gives our combined result.
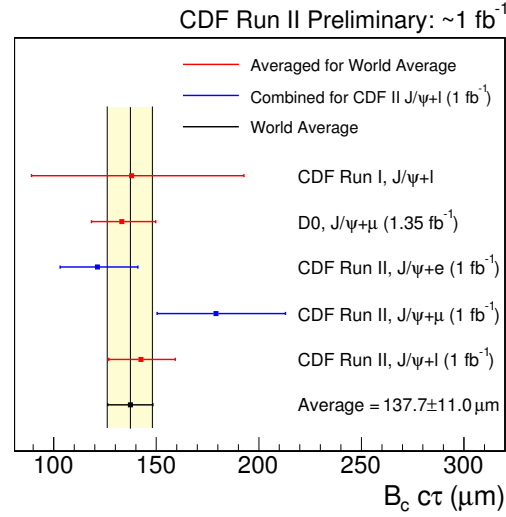
FIG. 18: Preliminary world average of B_c lifetime, which includes the CDF Run I B_c lifetime, the most recent D0 Run II result, and the result presented in this paper. The lifetimes are weighted by the total variance of the individual measurements in the average.

[1] V. V. Kiselev, arXiv:hep-ph/0308214.
[2] W. M. Yao *et al.* [Particle Data Group], J. Phys. G **33**, 1 (2006).
[3] F. Abe *et al.* [CDF Collaboration], Nucl. Instrum. Methods A **271**, 387 (1988). ; D. E. Amidei *et al.* (CDF Collaboration), Nucl. Instrum. Methods A **350**, 73 (1994). ; F. Abe *et al.* (CDF Collaboration), Phys. Rev. D **52**, 4784 (1995). ; P. Azzi *et al.*, Nucl. Instrum. Methods A **360**, 137 (1995). ; R. Blair *et al.* (CDF Collaboration), FERMILAB-PUB-96-390-E, (1996).
[4] A. Abulencia *et al.* (CDF Collaboration), Phys. Rev. Lett. **96**, 082002 (2006).
[5] A. Artikov *et al.*, Nucl. Instrum. Methods A **538**, 358 (2005).
[6] T. Affolder *et al.*, Nucl. Instrum. Methods A **526**, 249 (2004).
[7] A. Sill (CDF Collaboration), Nucl. Instrum. Methods A **447**, 1 (2000).
[8] A. Affolder *et al.* (CDF Collaboration), Nucl. Instrum. Methods A **453**, 84 (2000).
[9] C. Grozis *et al.* (CDF Collaboration), Int. J. Mod. Phys. A **16S1C**, 1119 (2001).
[10] T. Sjostrand, S. Mrenna and P. Skands, J. High Energy Phys. **0605**, 026 (2006).
[11] F. Abe *et al.* (CDF Collaboration), Phys. Rev. D **58**, 112004 (1998).
[12] http://www-d0.fnal.gov/Run2Physics/WWW/results/prelim/B/B52/B52.pdf.